frontiers in Marine Science

ORIGINAL RESEARCH
published: 18 February 2021
doi: 10.3389/fmars.2021.628363

Warming Iron-Limited Oceans Enhance Nitrogen Fixation and Drive Biogeographic Specialization of the Globally Important Cyanobacterium *Crocosphaera*

*Nina Yang[1], Carlin A. Merkel[1], Yu-An Lin[1], Naomi M. Levine[1,2], Nicholas J. Hawco[2†], Hai-Bo Jiang[3,4†], Ping-Ping Qu[1†], Michelle A. DeMers[1], Eric A. Webb[1], Fei-Xue Fu[1] and David A. Hutchins[1]**

[1] Department of Biological Sciences, University of Southern California, Los Angeles, CA, United States, [2] Department of Earth Sciences, University of Southern California, Los Angeles, CA, United States, [3] School of Life Sciences, Central China Normal University, Wuhan, China, [4] Southern Marine Science and Engineering Guangdong Laboratory, Zhuhai, China

Primary productivity in the nutrient-poor subtropical ocean gyres depends on new nitrogen inputs from nitrogen fixers that convert inert dinitrogen gas into bioavailable forms. Temperature and iron (Fe) availability constrain marine nitrogen fixation, and both are changing due to anthropogenic ocean warming. We examined the physiological responses of the globally important marine nitrogen fixer, *Crocosphaera watsonii* across its full thermal range as a function of iron availability. At the lower end of its thermal range, from 22 to 27°C, *Crocosphaera* growth, nitrogen fixation, and Nitrogen-specific Iron Use Efficiencies (N-IUEs, mol N fixed hour^{-1} mol Fe^{-1}) increased with temperature. At an optimal growth temperature of 27°C, N-IUEs were 66% higher under iron-limited conditions than iron-replete conditions, indicating that low-iron availability increases metabolic efficiency. However, *Crocosphaera* growth and function decrease from 27 to 32°C, temperatures that are predicted for an increasing fraction of tropical oceans in the future. Altogether, this suggests that *Crocosphaera* are well adapted to iron-limited, warm waters, within prescribed limits. A model incorporating these results under the IPCC RCP 8.5 warming scenario predicts that *Crocosphaera* N-IUEs could increase by a net 47% by 2100, particularly in higher-latitude waters. These results contrast with published responses of another dominant nitrogen fixer (*Trichodesmium*), with predicted N-IUEs that increase most in low-latitude, tropical waters. These models project that differing responses of *Crocosphaera* and *Trichodesmium* N-IUEs to future warming of iron-limited oceans could enhance their current contributions to global marine nitrogen fixation with rates increasing by ∼91 and ∼22%, respectively, thereby shifting their relative importance to marine new production and also intensifying their regional divergence. Thus, interactive temperature and iron effects may profoundly transform existing paradigms of nitrogen biogeochemistry and primary productivity in open ocean regimes.

Keywords: ocean warming, nitrogen fixation, iron limitation, iron use efficiency, *Crocosphaera*

OPEN ACCESS

Edited by:
Christopher Edward Cornwall, Victoria University of Wellington, New Zealand

Reviewed by:
Takako Masuda, Institute of Microbiology (ASCR), Czechia
Kristin M. Yoshimura, University of Delaware, United States

****Correspondence:***
David A. Hutchins
dahutch@usc.edu

†Present address:
Nicholas J. Hawco, Department of Oceanography, School of Ocean and Earth Sciences and Technology, University of Hawai'i at Mānoa, Honolulu, HI, United States
Hai-Bo Jiang, School of Marine Sciences, Ningbo University, Ningbo, China
Ping-Ping Qu, Department of Psychiatry and Behavioral Sciences, Stanford University School of Medicine, Stanford, CA, United States

Specialty section:
This article was submitted to Global Change and the Future Ocean, a section of the journal Frontiers in Marine Science

Received: *11 November 2020*
Accepted: *29 January 2021*
Published: *18 February 2021*

Citation:
Yang N, Merkel CA, Lin Y-A, Levine NM, Hawco NJ, Jiang H-B, Qu P-P, DeMers MA, Webb EA, Fu F-X and Hutchins DA (2021) Warming Iron-Limited Oceans Enhance Nitrogen Fixation and Drive Biogeographic Specialization of the Globally Important Cyanobacterium Crocosphaera. Front. Mar. Sci. 8:628363. doi: 10.3389/fmars.2021.628363

INTRODUCTION

Marine phytoplankton are important facilitators of biogeochemical cycling in the ocean, and contribute nearly half of the of the Earth's net primary production (Behrenfeld et al., 2006). Ocean warming threatens the stability and resiliency of marine ecosystems, and will undoubtedly also drive shifts in the distribution and activity of these keystone phytoplankton communities (Barton et al., 2016; Hutchins and Fu, 2017). In particular, temperature exerts significant influence over phytoplankton biogeography as a principal determinant of cellular biochemistry and metabolic processes, including growth and photosynthesis (Breitbarth et al., 2007; Huertas et al., 2011; Thomas et al., 2012; Boyd et al., 2013).

In the subtropical and tropical ocean gyres where large expanses of nutrient-poor surface waters persist, low concentrations of bioavailable nitrogen generally limit phytoplankton growth (Moore et al., 2013). In these regions, nitrogen-fixing cyanobacteria (N_2-fixers) or diazotrophs provide an essential ecosystem service by converting or "fixing" inert dinitrogen gas (N_2) into bioavailable ammonia (NH_3) that fuels primary productivity (Zehr et al., 2001; Sohm et al., 2011). While many microbial groups contribute to biological nitrogen fixation (N_2-fixation), cyanobacteria of the filamentous *Trichodesmium* and unicellular *Crocosphaera* genera are estimated to account for nearly half of the global total (Zehr and Capone, 2020). These two diazotrophic groups are key components of the marine nitrogen cycle and so, will help to determine how the availability of this limiting nutrient responds to ongoing changes in the ocean environment (Hutchins and Fu, 2017).

Culturing several strains of *Trichodesmium* and *Crocosphaera* across a range of temperatures has demonstrated that the two diazotrophs have differing thermal ranges for growth. *Trichodesmium* has a broader thermal range that can span from ∼18 to 32°C while *Crocosphaera's* range is narrower from ∼24 to 32°C (Fu et al., 2014). That study found that warmer temperatures within these thermal limits may enhance diazotrophic growth and N_2-fixation rates and also revealed that *Crocosphaera* may be better adapted to grow faster at warmer temperatures than *Trichodesmium* (Fu et al., 2014). However, because *Trichodesmium* and *Crocosphaera* are found in already-warm waters of ∼30°C, future ocean warming of ∼3.7°C under IPCC's "business as usual" RCP 8.5 scenario (IPCC, 2014) may surpass the thermal maxima of these N_2-fixers (∼35–36°C, Fu et al., 2014 and this study) and lead to their disappearance from some regions, with potentially negative implications for biogeochemistry across the low-latitude oceans (Breitbarth et al., 2007; Thomas et al., 2012).

The distribution, abundance, and function of these diazotrophs in open ocean regimes are likewise often constrained by the availability of the essential micronutrient iron (Fe), which is required as a cofactor for photosynthesis, respiration, and nitrogen-fixation enzymes (Moore et al., 2001; Schoffman et al., 2016). However, supplies of this essential micronutrient are insufficient to meet phytoplankton requirements in ∼40% of today's oceans (Moore et al., 2001, 2013), and are likely to be further altered in the future ocean by multiple global change processes (Hutchins and Boyd, 2016). To persist in low-Fe waters, N_2-fixers have evolved adaptive responses to acquire and efficiently use Fe under Fe-limiting conditions. For example, when Fe-limited, both *Trichodesmium* and *Crocosphaera* are able to substitute the iron-sulfur electron transport protein ferredoxin with iron-free flavodoxin (Roche et al., 1996; Chappell and Webb, 2010).

Previous studies have demonstrated that the two N_2-fixers differ in Fe requirements for their photosynthetic apparatus and for iron-rich nitrogenase, the metalloenzyme catalyst for N_2-fixation (Raven et al., 1999; Saito et al., 2011). This is in part due to differing strategies to protect their nitrogenase from oxygen, which inhibits its activity and consequently suppresses nitrogen fixation (Inomura et al., 2019). Thus, photosynthetic N_2-fixers that evolve oxygen as a byproduct must employ various strategies to partition photosynthesis and nitrogen fixation, which partly dictates their cellular iron requirements (Schoffman et al., 2016). *Trichodesmium* is capable of photosynthesizing while simultaneously fixing nitrogen, but at the cost of having higher cellular Fe requirements to maintain both metabolic pathways (Küpper et al., 2008; Saito et al., 2011). In contrast, *Crocosphaera* employs a repertoire of Fe-conservation strategies to reduce its cellular requirements relative to *Trichodesmium.* These include temporal separation of photosynthesis (day-time) and N2-fixation (night-time), daily synthesis and breakdown of metalloproteins to recycle Fe between the photosynthetic and N2-fixation metalloenzymes, and increased expression of flavodoxin at night (during N_2-fixation) even under Fe-replete conditions (Saito et al., 2011). In addition, *Crocosphaera* is better able to access dissolved Fe due to its smaller cell size and corresponding increase in the cell surface area-to-volume ratio compared to *Trichodesmium* (Finkel et al., 2010). Altogether, these strategies enable *Crocosphaera* to reduce its cellular Fe quota relative to *Trichodesmium* and allow *Crocosphaera* to outcompete *Trichodesmium* in Fe-scarce oligotrophic regimes (Saito et al., 2011). Thus, *Crocosphaera* may be the dominant N_2-fixer in regions of severe and chronic Fe-limitation, such as much of the Pacific Ocean. *Trichodesmium* occurs in greater abundance in areas like the North Atlantic, where episodic Saharan dust inputs alleviate Fe-limitation seasonally (Behrenfeld et al., 1996; Falkowski et al., 1998; Campbell et al., 2005; Sohm et al., 2011). How these distributions will respond to a warmer, Fe-limited future ocean is currently poorly understood.

Jiang et al. (2018) observed the interactive responses of *Trichodesmium* growth and N_2-fixation rates to warming relative to Fe availability (Jiang et al., 2018). They found that when *Trichodesmium* was Fe-limited, growth at warmer temperatures synergistically enhanced Nitrogen-specific Iron Use Efficiency (N-IUE, nitrogen fixation rate per unit Fe) by reducing cellular Fe requirements and increasing N_2-fixation rates. By applying their physiological measurements to IPCC's RCP 8.5 warming scenario for years 2010 and 2100, they projected a ∼76% increase in IUEs corresponding to a 21.5% increase in global marine N_2-fixation. Thus, warming may alleviate Fe-limitation for *Trichodesmium* across large expanses of the oligotrophic gyres in a warmer, future ocean (Jiang et al., 2018). It is unknown

whether *Crocosphaera* will exhibit similar responses to warming under low-Fe conditions.

In this study, we experimentally assess the interactive responses of *Crocosphaera* to warming under low-Fe conditions and use a modeling framework to incorporate our results and those of Jiang et al. (2018). We then use this approach to explore the impacts of a projected warmer ocean on the biogeographic distributions and biogeochemical functions of both *Trichodesmium* and *Crocosphaera* on a global scale.

MATERIALS AND METHODS

Culturing Methods

Triplicate cultures of *Crocosphaera watsonii* strain WH0005 were grown at five ecologically relevant temperatures spanning the thermal range of *Crocosphaera*: 20, 22, 27, 32, and 36°C. Cultures were maintained under two Fe conditions, Fe-replete and Fe-limited, in microwave-sterilized medium made with 0.2 μm-filtered surface seawater collected from the Sargasso Sea using a trace metal clean towfish system. The medium was amended with Aquil concentrations of phosphate (10 μM) passed through an activated Chelex 100 resin column (BioRad Laboratories, Hercules, CA, United States) to remove contaminating Fe, and with vitamins and a modified Aquil trace metals stock (1.21×10^{-7} M Mn, 7.97×10^{-8} M Zn, 1.00×10^{-7} M Mo, and 5.03×10^{-8} M Co) (Sunda et al., 2005). Fe-replete medium was amended with 250 nM Fe, while 5 nM was directly added to Fe-limited cultures during periodic dilutions. The media was buffered with 25 μM EDTA, and the resulting average concentration of dissolved free inorganic iron, which is the form most bioavailable to phytoplankton, was calculated for the different experimental conditions following Jabre and Bertrand (2020) (see **Supplementary Methods**, **Supplementary Table 1**, and **Supplementary Figure 1**). The Fe concentrations for the replete and limited media include the added Fe-EDTA, and a measured background Fe concentration in the Sargasso seawater of 0.54 nM (Held et al., 2020).

As in almost all laboratory studies, both the dissolved Fe and cell concentrations used in our culture experiments were necessarily higher than those found in the open ocean (Jiang et al., 2018). This Fe concentration increase in our culture experiments allows us to maintain a sufficient density of cells to carry out the required physiological measurements as well as molecular sampling for future analyses. Thus, the growth-limiting Fe concentration was determined as the concentration that would induce lower growth rates relative to the higher, replete growth Fe concentration, rather than concentrations expected from oligotrophic regimes.

Cultures were maintained semi-continuously in 2.5 L polycarbonate bottles on a 12:12 light:dark cycle in temperature-controlled incubators at 150 μmol photons m^{-2} s^{-1}, and diluted every three days with media adjusted to the experimental temperature to maintain steady-state exponential growth for at least 2 months. All bottles used in the study were soaked in a 1% Citranox detergent for 24 hours, rinsed in Milli-Q (18.2 Ω) water, and then soaked in 10% HCl for a week, rinsed in Milli-Q and microwave-sterilized before use. 0.2 μm filter-sterilized nutrients, trace metals, and vitamins were amended to the natural seawater base using sterile pipette tips rinsed three times with 1% HCl and three times with microwave sterilized Milli-Q water immediately prior to use.

Dilutions were conducted based on *in vivo* fluorescence measured in real-time on a 10AU Fluorometer (Turner Designs, San Jose, CA, United States). Cell samples were preserved in 0.5% 0.2-μm filtered glutaraldehyde to validate *in vivo* growth rates using on an Olympus BX51 epifluorescence microscope. The specific growth rate (μ) was then calculated using the equation $\mu = (\ln N_1 - \ln N_0)/t$, where N refers to cell densities and t is time in days. The cell size was determined by measuring the cell diameters of at least 20 cells per sample using the CaptaVision Imaging Software (Commack, NY, United States).

Elemental Stoichiometry

To measure particulate organic carbon and nitrogen (POC and PON), 30–40 mL of culture from each experimental treatment was filtered onto pre-combusted glass microfiber filters (Whatman, Grade GF/F), dried in an oven at ∼60°C, and then pelleted and analyzed on a 4010 Costech Elemental Analyzer calibrated with methionine and acetanilide (Jiang et al., 2018).

Nitrogen Fixation Rates

Nitrogen-fixation rates were measured using the acetylene reduction assay following previously described methods (Garcia et al., 2013). Briefly, duplicate 40 mL culture samples were collected from the triplicate experimental cultures and 6 mL of acetylene was injected into 35 mL of headspace at the start of the dark period in 75 mL sealed-top bottles. All-night (∼12 h) accumulation of acetylene was measured at the end of the incubation period on a gas chromatograph GC-8a (Shimadzu Scientific Instruments, Columbia, MD, United States), and the measured ethylene was converted to fixed N_2 using a ratio of 3:1 and a Bunsen coefficient of 0.086. Converted N_2-fixation rates were then normalized to particulate organic nitrogen (N-specific N_2-fixation rates).

Carbon Fixation Rates

To approximate net primary productivity (C-fixation), 10 mL sub-cultures from each experimental replicate were incubated for 5 h with $H^{14}CO_3$ beginning 2 h after the start of the light period under the same experimental growth conditions (e.g., light, temperature, etc.). Samples were then filtered onto glass microfiber filters (GF/F) and stored in the dark overnight before analysis using a Wallac System 1400 liquid scintillation counter (Jiang et al., 2018). Calculated rates were then normalized to particulate organic carbon (C-specific C-fixation rates).

Intracellular Iron Content

Intracellular Fe samples were obtained by filtering cultures onto acid-washed 0.2 μm Supor polyethersulfone filters (Pall

Laboratory) and rinsed with oxalate reagent to remove extracellular trace metals (Tovar-Sanchez et al., 2003). All filtration and sample processing steps were conducted in a class 100 trace metal clean environment. Filters were then digested with 5 mL of 50% nitric acid (HNO_3) amended with 10 ppb Indium as an internal standard at 95°C for 5 days in individual, 30 mL perfluoroalkoxy vials (Savillex). Following acid-digestion, the filters were removed with plastic tweezers, and samples were dried overnight at 100°C. Samples were resolubilized in 200 μL of 1:1 concentrated HNO_3 and hydrochloric acid (HCl), sealed, and heated for ∼2–3 h and then allowed to cool. The sample was dried and resuspended in 5 mL of 0.1 M distilled HNO_3 and then analyzed by inductively coupled plasma mass spectrometry (ICP-MS, Element 2, Thermo Fisher Scientific). Intensities of ^{56}Fe were calibrated with a 0.1–300 ppb metal reference standard curve. ^{115}In was monitored as an internal standard to correct for matrix suppression and any sample loss during digestion (Hawco et al., 2020). Two procedural blank filters for each treatment were also analyzed and subtracted from the measured sample values.

Fe Quotas and Resource Use Efficiencies

Iron quotas (mol Fe/μmol POC) were calculated using Fe concentrations measured via ICP-MS and POC (see above). N-IUEs were calculated by normalizing measured N_2-fixation rates to intracellular Fe content (mol N fixed h^{-1} mol cellular Fe^{-1}) (Kustka et al., 2003). Similarly, Carbon-specific Iron Use Efficiencies (C-IUEs, mol C fixed h^{-1} mol cellular Fe^{-1}) were calculated by normalizing measured C-fixation rates to intracellular iron.

Statistical Analyses

The significance of *Crocosphaera's* response to warming under Fe-replete and Fe-limited conditions for all reported physiological parameters was assessed via two-way ANOVA and a Tukey *post hoc* analysis at p-value <0.05.

Modeling Methods

We modeled *Crocosphaera* under Fe limitation and warming using two different models, an additive model and an interactive model, following Jiang et al. (2018). The additive model assumes that growth is independently affected by temperature and iron limitation whereby changes to one variable does not affect the other variable's impact on growth. While this is the traditional relationship used in biogeochemical models, recent studies have demonstrated interactive relationships between temperature and iron such that warming may influence phytoplankton iron use efficiency (Jiang et al., 2018; Jabre and Bertrand, 2020). Thus, our interactive model attempts to capture the observed multi-stressor impacts of Fe limitation and warming. For our additive model, we assumed a fixed half-saturation constant for Fe indicating that temperature did not affect Fe use. Our interactive model incorporates a flexible half-saturation constant that varies with temperature.

Additive Model

We assumed that Fe-limited growth followed Monod growth kinetics where growth rate (μ) is defined as (**Supplementary Figure 2**):

$$\mu_{\text{additive}} = \mu_{\text{T max}} \frac{[\text{Fe}]}{[\text{Fe}] + \text{Ksp}_{\text{Croco}}} \quad (1)$$

μ_{Tmax} is the calculated maximum growth rate (see Eqs 3 and 5), and [Fe] is the iron concentration. Ksp_{Croco} is the fixed half-saturation constant for iron under the optimal growth temperature (27°C) calculated by deriving Eq. 1 to set μ_{Tmax} of replete and limited growth as equal, and then solving for Ksp_{Croco}:

$$\text{Ksp}_{\text{Croco}} = \frac{(\text{Fe}_{\text{limit}}\text{Fe}_{\text{replete}})(\mu_{\text{replete}} - \mu_{\text{limit}})}{(\text{Fe}_{\text{replete}}\mu_{\text{limit}} - \text{Fe}_{\text{limit}}\mu_{\text{replete}})} \quad (2)$$

where replete and limit subscripts denote the Fe-limited and replete experimental conditions for Fe concentrations and growth rates (μ) at 27°C.

The temperature dependence for growth rate was estimated by calculating μ_{Tmax} for each experimental temperature as:

$$\mu_{\text{Tmax}} = \frac{\mu_{\text{replete}}(\text{Fe}_{\text{replete}} + \text{Ksp}_{\text{T}})}{\text{Fe}_{\text{replete}}} \quad (3)$$

where Ksp_T is the calculated Ksp at each experimental temperature using a similar equation to Eq 2:

$$\text{Ksp}_{\text{T}} = \frac{(\text{Fe}_{\text{Tlimit}}\text{Fe}_{\text{Treplete}})(\mu_{\text{Treplete}} - \mu_{\text{Tlimit}})}{(\text{Fe}_{\text{Treplete}}\mu_{\text{Tlimit}} - \text{Fe}_{\text{Tlimit}}\mu_{\text{Treplete}})} \quad (4)$$

Treplete and Tlimit subscripts denote the Fe-limited and replete experimental conditions for Fe concentrations and growth rates (μ).

Calculated μ_{Tmax} rates were then fit to a polynomial curve to model temperature limited growth (Breitbarth et al., 2007) (**Supplementary Figure 3A**):

$$\mu_{\text{Tmax}} = -0.005816\text{T}^2 + 0.32290\text{T} - 4.13443 \quad (5)$$

μ_{Tmax} was bounded by the experimental thermal response norm with growth rates below 20°C and above 36°C set to 0.

Since the Fe concentrations used in the culture study were higher than that found naturally in oligotrophic regimes, the Ksp values calculated from these cultures are correspondingly higher than Ksps in the ocean. To reconcile this discrepancy, both Ksp_{Croco} and the calculated temperature-dependent Ksps (Ksp_T) were scaled down to convert Fe concentrations used in our biomass-dense cultures to those reflective of open-ocean conditions as in Jiang et al. (2018). In that study with *Trichodesmium*, a similar Fe scaling factor (α_{Fe_Tricho}) was calculated as the ratio of the Ksp of *in situ Trichodesmium* (Ksp_{field}) based on a pre-established threshold of ∼0.33 nM Fe for isiB (Fe stress biomarker) gene expression, and the Ksp at the optimal growth temperature in culture. As the Ksp_{field} is unknown for *Crocosphaera*, the effective Fe concentration used in our modeling input was based on a modified scaling factor for *Crocosphaera* (α_{Fe_Croco}) calculated using the *Trichodesmium* Fe

scaling factor (α_{Fe_Tricho} = 0.02564, Jiang et al., 2018) and the ratios of the Ksp values under optimal growth conditions for *Crocosphaera* (2.4 nM, Eq. 2) and *Trichodesmium* (12.9 nM, Jiang et al., 2018):

$$\alpha_{\mathrm{Fe\_Croco}} = \alpha_{\mathrm{Fe\_Tricho}} \frac{\mathrm{Ksp_{Croco}}}{\mathrm{Ksp_{Tricho}}} = 0.00478 \quad (6)$$

α_{Fe_Croco} was used to convert all experimentally derived Ksp values (Ksp_{Croco} and Ksp_T for each experimental temperature) so that they could be used with model outputs. To verify this scaling exercise, we can use the POC:dissolved Fe ratio as a simple proxy for relative Fe availability to the algal cells in order to compare the values in our cultures with field samples. The ratio of *Crocosphaera* biomass to total Fe added (POC:dissolved Fe) in our limited cultures under the optimum growth temperature of 27°C was calculated to be 4.26×10^4 mol:mol, which roughly corresponds to the calculated POC:dFe ratio of 3.64×10^4 based on oligotrophic POC field data (Martiny et al., 2013) and a dissolved Fe concentration of 0.11 nM, which is reasonable for low-Fe regimes (Jiang et al., 2018). See **Supplementary Material** for further discussion on scaling Fe quota values.

Interactive Model

The interactive model replaced Ksp_{Croco} in Eq 1 with Ksp_{Ti}, the temperature dependent half saturation constant, in order to capture the interactive effect of Fe limitation and warming.

$$\mu_{\mathrm{interactive}} = \mu_{\mathrm{Tmax}} \frac{[\mathrm{Fe}]}{[\mathrm{Fe}] + \mathrm{Ksp_{Ti}}} \quad (7)$$

The interactive relationship between the calculated Ksp_T (Eq. 4) and temperature (T) was then estimated as the best polynomial fit to the data, Ksp_{Ti} (**Supplementary Figure 3B**):

$$\mathrm{Ksp_{Ti}} = 0.00018\mathrm{T}^2 - 0.01049\mathrm{T} + 0.161015 \quad (8)$$

Modeling N_2-Fixation Rates

A linear relationship was used to relate N_2-fixation and growth when modeling *Trichodesmium* N_2-fixation rates in Jiang et al., 2018 (Hutchins et al., 2013; Jiang et al., 2018). For *Crocosphaera*, N_2-fixation rates (fmol N h^{-1} $cell^{-1}$) and cell-specific growth rates across all growth temperature and Fe experimental conditions were measured at four time points during steady-state exponential growth to establish the linear relationship using a two-way least squares fit between the two rates under varying temperature and Fe availability (**Supplementary Figure 4**).

$$\text{Nitrogen fixation} = 18.022\mu - 0.1923 \quad (9)$$

Interactive or additive effects of temperature and Fe on N_2-fixation are thus determined by either additive or interactive growth (μ).

Modeling Iron Use Efficiencies (IUEs)

Nitrogen-specific Iron Use Efficiencies were determined as in Jiang et al. (2018). Briefly, calculated N-IUEs from each temperature treatment were linearly related to the scaled Fe concentration (**Supplementary Figure 5A**). Then, the N-IUE slope (m) and intercepts (b) were individually related to temperature via a best polynomial fit to establish the impact of temperature (T) on the relationships between the slope (m) and intercepts (b) of calculated IUEs and the scaled Fe concentration (**Supplementary Figures 5B,C**). The maximum modeled response for m outside of the experimental growth temperatures (22, 27, and 32°C) was set to 13.4616 while the minimum modeled response for b was set to 5.1718.

$$m = 2.3195\mathrm{T}^2 - 126.6903\mathrm{T} + 1672.5701 \quad (10)$$

$$b = -5.2694\mathrm{T}^2 + 289.2894\mathrm{T} - 3808.7982 \quad (11)$$

Finally, N-IUE was estimated as a linear function of Fe concentration and temperature where m is slope represented by Eq. 10, b is the intercept represented by Eq. 11, and $[Fe]$ is the scaled Fe concentration.

$$N - IUE = m[Fe] + b \quad (12)$$

RESULTS

The thermal optimum for *Crocosphaera* growth under both Fe-replete and Fe-limited treatments was at 27°C, with the thermal minimum and maximum at 20 and 36°C, respectively. As expected, under Fe-limitation *Crocosphaera* growth rates were significantly lower relative to Fe-replete cultures across experimental temperatures of 22, 27, and 32°C where cultures exhibited active growth (**Figure 1**). In addition, growth at 32°C (supra-optimum) was significantly higher than growth at 22°C (sub-optimum). At the optimum growth temperature of 27°C, both Fe-replete and Fe-limited cells had significantly smaller diameters than cells growing at 22°C (**Supplementary Figure 6**).

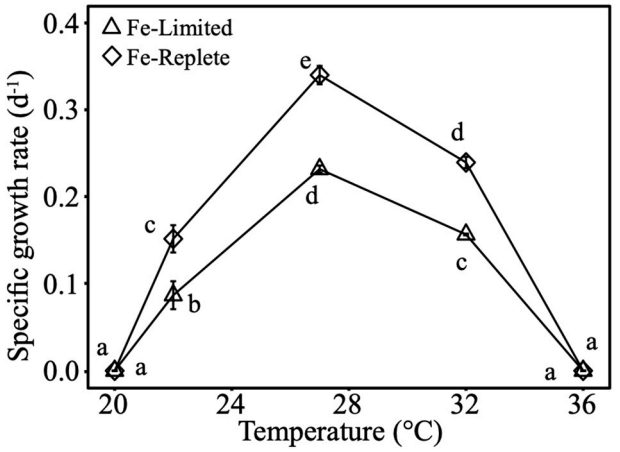

FIGURE 1 | Cell-specific growth rates of *Crocosphaera* grown under Fe-replete and Fe-limited conditions across 5 temperatures (20, 22, 27, 32, and 36°C) that span their thermal range. Error bars are standard deviations of the means of triplicates, and different letters represent statistical significance between growth rate means at p-value <0.05.

In addition, under Fe-limited conditions, cell diameter was larger at 32°C than 27°C.

Calculated N-IUEs (mol N fixed h^{-1} mol intracellular Fe^{-1}), showed that at the optimal growth temperature of 27°C, Fe-limited N-IUE increased by 66% relative to Fe-replete cultures (**Figure 2A**). N-IUEs were not significantly different between Fe treatments at 22°C (sub-optimum) and 32°C (supra-optimum) (p-value >0.05), although 22°C N-IUEs exhibited a 64% decrease between replete and limited cultures. *Crocosphaera* N-IUE increased significantly from the cooler temperature to the optimum N-IUE temperature, especially under Fe-limiting conditions where N-IUE increased by nearly 141% from 22 to 27°C (**Figure 2A**).

Carbon-specific-IUEs (C-IUEs, mol C fixed h^{-1} mol intracellular Fe^{-1}) exhibited similar patterns to N-IUEs, such that C-IUEs were also highest at the growth thermal optimum (27°C), with higher IUEs under Fe-limiting conditions (**Figure 2B**). The minimum C-IUE for both Fe treatments occurred at 22°C. The increase from 22 to 27°C for Fe-replete cultures was 280%, and the IUE differential was even higher under Fe-limiting conditions, with an increase of >1,600%. Again, like N-IUEs, C-IUEs dropped from 27 to 32°C by 65–68% for Fe-limited and Fe-replete cultures, respectively (**Figure 2B**).

Similar to growth rates, *Crocosphaera* N-specific N_2-fixation rates (h^{-1}) were significantly lower under Fe-limiting relative to Fe-replete conditions. As with IUEs, there was also a trend of increases in N_2-fixation rates from 22 to 27°C. Regardless of Fe availability, N_2-fixation rates were lowest at 22°C while cultures grown at the warmer temperatures (27 and 32°C) had the highest rates, ranging from 338 to 388% higher under Fe-limiting conditions (**Figure 2C**).

C-fixation rates (h^{-1}) significantly decreased between Fe-replete and Fe-limited cultures at 22°C, whereas at the warmer temperatures of 27°C and 32° Fe-limited rates were comparable to Fe-replete rates (**Figure 2D**). Consistent with the other three metabolic parameters, Fe-limited cultures also exhibited a significant temperature-driven increase in C-fixation rates of 332% between 22 and 27°C. However, at the higher end of their thermal range (27 to 32°C), Fe-limited C-fixation rates decreased significantly from 27 to 32°C by nearly 14.5% (**Figure 2D**).

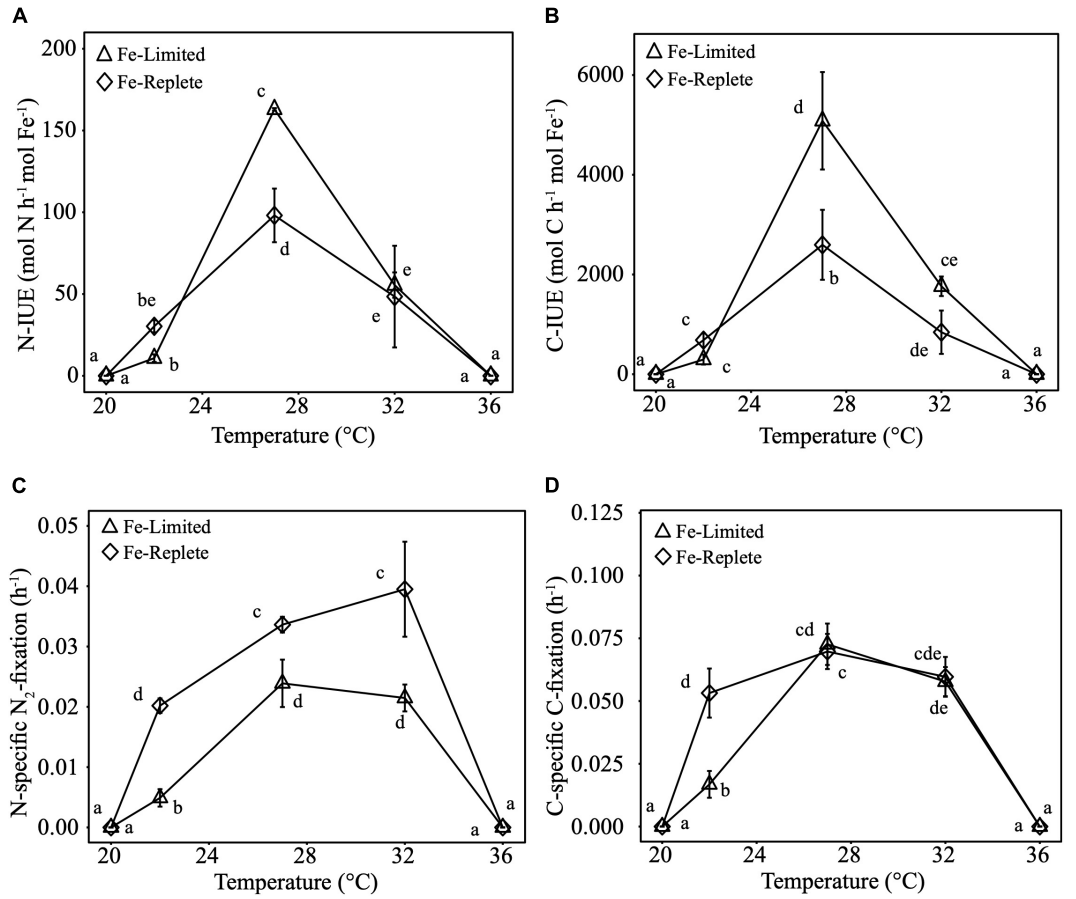

FIGURE 2 | Nitrogen-specific Iron Use Efficiencies (N-IUEs, mols of N fixed h^{-1} mol intracellular Fe^{-1}) **(A)**, Carbon-specific Iron Use Efficiencies (C-IUEs, mols of C fixed h^{-1} mol intracellular Fe^{-1}) **(B)**, Nitrogen-specific nitrogen fixation rates (h^{-1}) **(C)**, and Carbon-specific carbon fixation rates (h^{-1}) **(D)** of *Crocosphaera* grown in triplicate under Replete and Limited iron conditions at 20, 22, 27, 32, and 36°C. Error bars are standard deviations from the mean and different letters represent statistical significance between mean values at p-value <0.05.

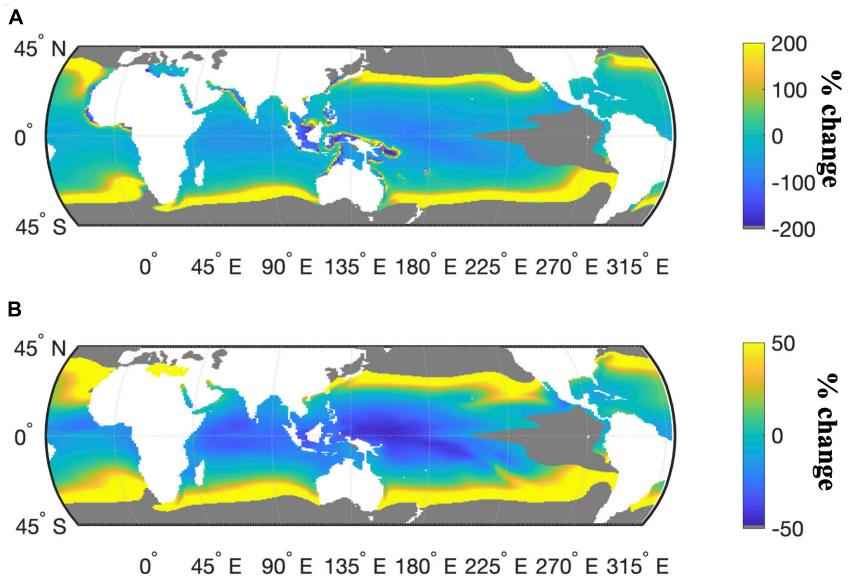

FIGURE 3 | Percent change in the modeled response of *Crocosphaera* N-IUE (mol N fixed h^{-1} mol Fe^{-1}) **(A)** and N_2-fixation (fmol N h^{-1} $cell^{-1}$) **(B)** for the years 2010 and 2100 under the IPCC RCP 8.5 warming scenario. Gray masked areas exclude areas where nitrate concentrations are >5 μM or where temperatures are outside the thermal range, and where modeled growth rates are consequently assumed to be negligible (<0.01 day^{-1}).

To place these culture-based results in a global context, we modeled N_2-fixation and N-IUE using the experimentally derived equations as a function of temperature and Fe (see section "Materials and Methods"). National Center for Atmospheric Research (NCAR) Community Earth System Model (CESM) projected Fe concentrations and temperatures under the IPCC RCP 8.5 "business-as-usual" emissions scenario were then applied to these equations to model global N_2-fixation and N-IUE outputs. Model results projected an average global increase of 47% in *Crocosphaera* N-IUEs from 2010 to 2100, with some regions experiencing increases that exceeded 1,300%, particularly the higher latitudes bordering the subtropical oceans (**Figure 3A**, sensitivity analysis in **Supplementary Figure 7**). The average global N-IUEs increases also included decreases of over 183% in some of the warmest regions of the tropics, such as the western Pacific and the central Indian Ocean. The model projected that *Crocosphaera* N_2-fixation rates will increase globally in 2100 by 91% on average, but with similarly large regional differences (**Figure 3B**, sensitivity analysis in **Supplementary Figure 8**). The largest increases were concentrated in the higher latitudes bordering the central gyres, areas where current temperatures are well below *Crocosphaera's* thermal growth optimum and likewise constrain IUEs (**Figure 3A**). Conversely, the low-latitude tropical oceans where future warming will likely exceed *Crocosphaera's* thermal range and reduce IUEs will also experience decreased rates of N_2-fixation by this cyanobacterium (**Figure 3B**).

DISCUSSION

Our study demonstrates that temperature may be an important determinant of Iron Use Efficiency and Fe-dependent metabolism in *Crocosphaera*, with important implications for global biogeochemistry in a warming ocean. Low temperatures may reduce enzyme activity and impede metabolic functions, constraining some diazotrophs to the warm subtropical and tropical oceans (Webb et al., 2009; Sohm et al., 2011; Fu et al., 2014). For example, decreased respiration rates reduce the ability to remove intracellular O_2, which can directly inhibit N_2-fixation (Inomura et al., 2019). Similarly, one study on the unicellular N_2-fixing cyanobacterium *Cyanothece* suggested that low temperature may impede the onset of N_2-fixation, due to possible delays in *de novo* synthesis of functional nitrogenases for night-time N_2-fixation (Brauer et al., 2013). Thus, thermal rate enhancement of key metabolic processes may be an important response mechanism to compensate for Fe limitation in low-Fe oceanic regimes.

Warmer temperatures may enhance photosynthesis and respiration in *Crocosphaera*, which could in turn indirectly promote N_2-fixation (Raven and Geider, 1988; Großkopf and LaRoche, 2012; Inomura et al., 2019), perhaps by helping to offset the energy costs of daily degradation and *de novo* synthesis of nitrogenase. In fact, maintaining photosynthetic function may be a key aspect of retaining N_2-fixing capabilities by providing carbon for respiration, which supplies energy necessary for nitrogenase function. N_2-fixation is a notoriously slow, energy-intensive process requiring 16 ATP to reduce one molecule of N_2 into two molecules of ammonia (Sohm et al., 2011).

Previous studies have suggested that both temperature (Finkel et al., 2010) and nutrient stress (Peter and Sommer, 2013) may cause a reduction in phytoplankton cell size. Furthermore, it has been shown that *Crocosphaera* will reduce its cell size under Fe-limiting growth conditions (Jacq et al., 2014). A smaller cell size and thus, a larger surface area-to-volume ratio, is beneficial for

Crocosphaera under Fe stress because it enables better access to Fe relative to larger cells. Our results indicated that warming may significantly reduce cell size, with *Crocosphaera* growing at 27°C measuring significantly smaller than cells growing at 22°C. In addition, we also saw a small nutrient stress effect whereby Fe-limited cells at 27°C were slightly smaller than replete cells at the same growth temperature. These patterns of temperature and Fe-induced cell size reduction at 27°C may contribute to the enhanced IUEs observed for Fe-limited *Crocosphaera*. Surprisingly, cell size actually increased from 27 to 32°C. *Crocosphaera* cell size varies through its cell cycle which can be affected by cell division, photosynthesis, and carbon catabolism to power N_2-fixation (Dron et al., 2012). While this response may have important implications for *Crocosphaera* function at the upper bound of its thermal range, the mechanisms underlying this response remain poorly investigated.

We compared the physiological parameters measured for *Crocosphaera* against the responses of *Trichodesmium* reported by Jiang et al. (2018). Both *Trichodesmium* and *Crocosphaera* exhibited the slowest growth and lowest N_2-fixation and C-fixation rates at 22°C, with Fe-limitation driving further significant decreases in growth and function. However, under warmer temperatures, a thermally driven alleviation of Fe-limitation was observed in both diazotrophs, albeit in contrasting ways. For example, *Trichodesmium* exhibited higher N-IUEs at 32°C that corresponded with a shift in the thermal optimum for N_2-fixation from 27°C under Fe-replete conditions to 32°C under Fe-limited conditions, indicating an interactive effect between warming and low-Fe availability that may offset Fe limitation to enhance function (**Supplementary Figure 9**; Jiang et al., 2018). In contrast, *Crocosphaera* N_2-fixation and IUE thermal optima did not shift, and instead remained constant at 27°C. However, at this thermal optimum, *Crocosphaera* IUEs were much higher under Fe-limited conditions relative to Fe-replete conditions. By comparison, Fe-limitation led to significant decreases in *Trichodesmium* IUE across all experimental temperatures, likewise suggesting an interactive effect of temperature and Fe-limitation in enhancing IUE.

It is possible that the higher IUEs for Fe-limited *Crocosphaera* relative to the Fe-replete cultures are influenced by luxury uptake of Fe under replete conditions. Thus, for replete cultures, the calculated IUEs can be considered a minimum IUE estimate. However, the same trend is not seen for *Trichodesmium,* where Fe-limited cultures exhibited lower IUEs across the three experimental temperatures compared to Fe-replete cultures (Jiang et al., 2018), suggesting that additional mechanisms besides luxury uptake need to be considered.

These differences in diazotrophic IUEs appear to drive the varying responses of Fe-limited N_2-fixation and C-fixation rates to warming. *Trichodesmium* N_2-fixation and C-fixation rates follow a similar pattern to growth in response to temperature and Fe-limitation, such that the rates increase in a step-wise manner as a function of temperature with a thermal optimum at 32°C, where N-IUE and C-IUE were also highest (Jiang et al., 2018). For *Crocosphaera,* while IUEs were significantly higher at 27°C than at 32°C, N_2-fixation and C-fixation rates were comparable at those temperatures. It is unclear why these rates do not reflect the responses of growth or IUE to Fe-limitation and warming. Higher concentrations of intracellular iron (Fe quotas) at 32°C relative to 27°C under both Fe-replete and Fe-limiting conditions suggest that metabolic rates may be maintained at the expense of increasing intracellular Fe requirements (**Supplementary Table 2**). One possibility is lower biodilution rates of cellular Fe, whereby Fe uptake rates might be unchanged while growth rates are slowed at 32°C relative to 27°C, resulting in higher cellular Fe quotas.

Another potential explanation is that warming beyond *Crocosphaera's* optimal growth temperature disrupts the Fe-conserving diel patterns of photosynthetic and N_2-fixing enzyme synthesis and degradation, thereby increasing the cellular Fe demand required to maintain functionality. This temperature-induced disruption could also prompt changes to protein expression that enable *Crocosphaera* to maintain photosynthetic activity and drive N_2-fixation. For example, Saito et al. (2011) noted that when Fe-limited, *Crocosphaera* seemingly increases the abundance of proteins involved in C-fixation, which indicates the existence of mechanisms that increase C-fixation efficiency under stress (Saito et al., 2011). While the mechanisms of *Crocosphaera* warming responses are unknown, warmer temperatures in conjunction with limited Fe availability may interactively influence protein abundance and activity patterns that underlie our observed physiological trends. *Trichodesmium* is unique in its ability to simultaneously photosynthesize while fixing N_2 and has thus developed strategies that may benefit from increased temperatures under Fe-limitation. These include both spatial and temporal sequestration of nitrogenase and N_2-fixation throughout the photoperiod (Bergman et al., 2013). More work is needed to better understand the mechanistic underpinnings of thermally enhanced metabolic rates at the expense of higher Fe requirements.

The incorporation of experimental data into quantitative models allows us to better understand the impacts of warming on diazotroph function on a global scale, and to evaluate the potential biogeochemical implications in a future, warmer ocean scenario. Here we compare the predictions of an additive model and an interactive model using experimentally observed relationships between Fe availability and temperature on IUE and metabolic rates. Our results generated from an interactive model show that ocean warming projected under IPCC's RCP 8.5 scenario may alleviate prevailing Fe-limitation of N_2-fixation by the globally important diazotrophs *Trichodesmium* and *Crocosphaera* throughout much of the world's oligotrophic oceans, with N_2-fixation rates increasing by ∼22% (Jiang et al., 2018) and 91%, respectively. Under projected future ocean conditions, the additive and interactive models largely predict similar *Crocosphaera* N_2-fixation rates across the global subtropical and tropical oceans with a <1% average difference between the two models (**Supplementary Figure 10A**). The small difference between the two projections was driven by slightly higher N_2-fixation rates projected by the additive model compared to the interactive model in regions where water temperatures were either above (equatorial Pacific) or below (high-latitudes) *Crocosphaera's* thermal optimum. This is in contrast to the published *Trichodesmium* response showing that

the additive effects of temperature and iron were lower than the synergistic interactive effects, especially in the equatorial Pacific where warm temperatures enhanced N_2-fixation rates (Jiang et al., 2018; **Supplementary Figure 10B**). Regardless of the modeling approach used, it is clear that warming enhances N_2-fixation despite Fe scarcity, resulting in significant increases of new nitrogen input across the Fe-limited oceans. Moreover, due to a projected near doubling of *Crocosphaera* nitrogen fixation rates under future conditions, *Crocosphaera's* contribution to global nitrogen fixation may increase relative to *Trichodesmium* in the future. Collectively, these results suggest that although the current low latitude oceans are predominantly nitrogen-limited (Moore et al., 2013), thermal rate enhancement of diazotrophy may help to alleviate this stress, even when Fe is also limiting or co-limiting with nitrogen.

To assess the biogeographical implications of the distinct *Trichodesmium* and *Crocosphaera* responses to Fe-limitation and warming, we compared the interactive model outputs for the percent changes in N-IUE and N_2-fixation from 2010 to 2100. These are based on the assumption that physiological responses depend on Fe-availability and vary as a function of temperature. Since the magnitude of change is different between the two diazotrophs, we used quartiles to identify regions with the largest change for each group. Here we present results using the 75% quartile (top 25%), but the conclusions are independent of this threshold (**Supplementary Figures 11,12**). **Figure 4A** shows the regions where the N-IUE percent change from 2010 to 2100 for *Crocosphaera* and *Trichodesmium* were within this top quartile. Minimal overlap occurs for N-IUEs, indicating a niche differentiation in thermal responses and Fe requirements that could drive spatial divergence between these two diazotrophs in the future. In a warmer ocean scenario, *Trichodesmium* is most dominant in the Fe-limited tropical oceans, as the greatest increases in its IUEs occur at the upper end of its thermal range, from 27 to 32°C (Jiang et al., 2018). In contrast, IUEs in *Crocosphaera* increase most in the lower portion of its thermal curve, from 22 to 27°C, facilitating its range expansion into the newly warmed higher latitudes. Thus, taxon-specific changes to IUEs directly influence the prevalence and patterns of N_2-fixation. Coincidentally, the contrasting thermal responses of both groups lead to net diazotrophic IUE increases that encompass virtually the entire basins of the oligotrophic oceans where conditions are otherwise suitable for N_2-fixation (i.e., where temperatures and nitrate levels remain below critical thresholds, **Figure 4A**).

A similar assessment using projected increases in N_2-fixation shows a parallel trend of future latitudinal partitioning between the two nitrogen fixers (**Figure 4B**). In this analysis, the regions of overlap are more expansive between *Trichodesmium* and *Crocosphaera,* suggesting a potential for competition. However, based on our N-IUE analysis it is likely that *Crocosphaera* may emerge as the winner in the higher latitude oceans, since projected temperatures at those latitudes increase to near *Crocosphaera's* thermal optimum.

It is important to note that while our analysis highlighted regions where net thermally enhanced N_2-fixation rates are predicted to occur, our models also identified regions where ocean warming may exceed the thermal optimum of *Crocosphera* and result in negative changes to N_2-fixation rates in the future. These patterns can be found in the individually modeled response for both diazotrophs as well as in the overlap analysis. Whereas *Trichodesmium* function may decrease across parts of the western

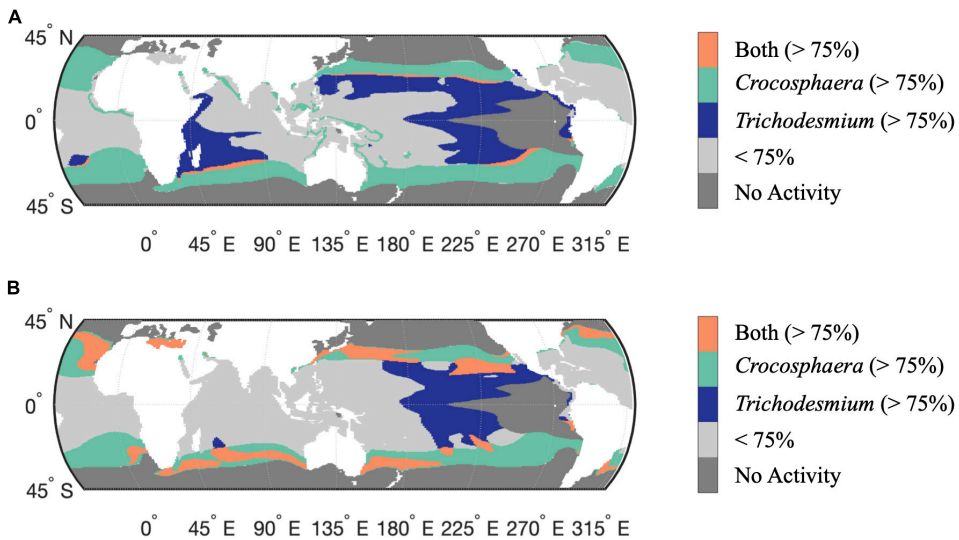

FIGURE 4 | Comparative change in the modeled responses of *Crocosphaera* and *Trichodesmium* N-IUE **(A)** and N_2-fixation **(B)** for the years 2010 and 2100 under the IPCC RCP 8.5 warming. Colored areas mark where the percent change in physiology is predicted to increase the most (above the 75% quantile) for either diazotroph, green (*Crocosphaera*) and purple (*Trichodesmium*) with the overlap between the two diazotrophs colored in orange. Light gray masked areas mark areas where activity is below the 75% quantile for either diazotroph. Gray masks regions of assumed no activity where nitrate concentrations are >5 μM or where temperatures are outside the thermal range, and where modeled growth rates are consequently assumed to be negligible (<0.01 day^{-1}).

Equatorial Pacific as well as the Indian Ocean (Jiang et al., 2018), our study found that *Crocosphaera* may experience decreases in N_2-fixation throughout the tropical low-latitude oceans as water temperature greater than 27°C become an increasingly prevalent feature across this region.

Of course, changes in cell-specific rates are only one part of the equation in determining overall changes to global new nitrogen inputs; we also need to consider overall and group-specific diazotroph biomass in the context of regional temperature-driven changes. However, in both *Crocosphaera* and *Trichodesmium*, increases in N_2-fixation rates such as those observed and modeled here are closely linearly correlated with higher growth rates (**Supplementary Figure 4**; Hutchins et al., 2013; Jiang et al., 2018), and thus potentially with biomass increases as well. Our current model does not resolve the net change to diazotroph biomass between 2010 and 2100 and references the trends in N-IUEs and N_2-fixation rates as a proxy for net new nitrogen input. Including a biomass parameter through the use of *nifH* genes to quantify group-specific marine diazotroph biomass could be an illuminating parameter in future iterations of this modeling exercise.

While our culture experiments and model analysis focused on temperature and Fe availability, other important constraints on diazotrophic cyanobacteria including phosphate (P) limitation and Fe/P co-limitation should also be considered (Moore et al., 2013; Zehr and Capone, 2020). Studies have shown that Fe availability influences the nitrogen and phosphorus cycles (Browning et al., 2017). If warming changes iron use efficiency, then it will also change the interactions with these other cycles in currently unknown ways. Ocean warming necessitates a deeper understanding of the interacting effects of temperature and all other major drivers of primary productivity. Only when this is achieved can we quantify the net impacts of these environmental drivers on microbially mediated biogeochemistry. In this study, we incorporated our experimental observations into global projections for N-IUE and N_2-fixation rates that revealed potential implications for the marine nitrogen cycle in a warmer, Fe-limited ocean. By comparing the model results of *Crocosphaera* and *Trichodesmium*, we found that genus-specific responses of the two cyanobacterial N_2-fixers may alter existing spatiotemporal patterns of marine nitrogen fixation and thus, the regional availability of limiting nutrients in the future oligotrophic ocean. These thermally driven shifts in diazotroph biogeography, and the accompanying overall increases in future global marine N_2-fixation, may profoundly transform existing patterns of biological productivity and Fe and nitrogen biogeochemistry in open ocean regimes. Additional research efforts are needed to uncover the molecular underpinnings of these response mechanisms and provide more accurate predictions of diazotroph distributions and activity changes due to future ocean warming.

DATA AVAILABILITY STATEMENT

The datasets presented in this study can be found in online repositories. The names of the repository/repositories and accession number(s) can be found below: https://www.bco-dmo.org/search/dataset/Hutchins.

AUTHOR CONTRIBUTIONS

F-XF and DH conceived and designed the experiments with help from NY. NY carried out the experiments, with significant help from CM and Y-AL in monitoring cultures using cell-based growth rates. MD, H-BJ, EW, and F-XF also contributed to the experimental maintenance. NY, H-BJ, NH, and P-PQ conducted the physiological measurements and data analyses. NY and NL carried out the modeling analyses. NY wrote the manuscript with critical contributions from NL, NH, EW, F-XF, and DH. All authors reviewed and gave their approval for the final manuscript.

FUNDING

This research was supported by U.S. National Science Foundation Biological Oceanography program grants OCE 1260490, OCE 1657757 and OCE 1851222 to DH, F-XF, and EW, OCE 1538525 to F-XF, DH, and NL, Simons Foundation Postdoctoral Fellowship 602538 to NH, as well as graduate student support from a USC Provost Fellowship to NY.

SUPPLEMENTARY MATERIAL

The Supplementary Material for this article can be found online at: https://www.frontiersin.org/articles/10.3389/fmars.2021.628363/full#supplementary-material

REFERENCES

Barton, A. D., Irwin, A. J., Finkel, Z. V., and Stock, C. A. (2016). Climate change drives shift and shuffle in north atlantic phytoplankton communities. *Proc. Natl. Acad. Sci. U S A.* 113, 2964–2969. doi: 10.1073/pnas.1519080113

Behrenfeld, M. J., Bale, A. J., Kolber, Z. S., Aiken, J., and Falkowski, P. G. (1996). Confirmation of iron limitation of phytoplankton photosynthesis in the equatorial pacific ocean. *Nature* 383:508. doi: 10.1038/383508a0

Behrenfeld, M. J., O'Malley, R. T., Siegel, D. A., McClain, C. R., Sarmiento, J. L., Feldman, G. C., et al. (2006). Climate-driven trends in contemporary ocean productivity. *Nature* 444:752. doi: 10.1038/nature05317

Bergman, B., Sandh, G., Lin, S., Larsson, J., and Carpenter, E. J. (2013). *Trichodesmium*–a widespread marine cyanobacterium with unusual nitrogen fixation properties. *FEMS Microbiol. Rev.* 37, 286–302. doi: 10.1111/j.1574-6976.2012.00352.x

Boyd, P. W., Rynearson, T. A., Armstrong, E. A., Fu, F., Hayashi, K., Hu, Z., et al. (2013). Marine phytoplankton temperature versus growth responses from polar to tropical waters - outcome of a scientific community-wide study. *PLoS One* 8:e63091. doi: 10.1371/journal.pone.0063091

Brauer, V. S., Stomp, M., Rosso, C., van Beusekom, S. A. M., Emmerich, B., Stal, L. J., et al. (2013). Low temperature delays timing and enhances the cost of nitrogen fixation in the unicellular cyanobacterium *Cyanothece*. *ISME J.* 7:2105. doi: 10.1038/ismej.2013.103

Breitbarth, E., Oschlies, A., and LaRoche, J. (2007). Physiological constraints on the global distribution of *Trichodesmium*: effect of temperature on diazotrophy. *Biogeosciences* 4, 53–61. doi: 10.5194/bg-4-53-2007

Browning, T. J., Achterberg, E. P., Yong, J. C., Rapp, I., Utermann, C., Engel, A., et al. (2017). Iron limitation of microbial phosphorus acquisition in the tropical north atlantic. *Nat. Commun.* 8:15465. doi: 10.1038/ncomms15465

Campbell, L., Carpenter, E., Montoya, J., Kustka, A., and Capones, D. (2005). Picoplankton community structure within and outside a *Trichodesmium* bloom in the southwestern pacific ocean. *Vie. Milieu Paris* 55, 185–195.

Chappell, P. D., and Webb, E. A. (2010). A molecular assessment of the iron stress response in the two phylogenetic clades of *Trichodesmium*. *Environ. Microbiol.* 12, 13–27. doi: 10.1111/j.1462-2920.2009.02026.x

Dron, A., Rabouille, S., Claquin, P., Le Roy, B., Talec, A., Sciandra, A. et al. (2012). Light-dark (12:12) cycle of carbon and nitrogen metabolism in *Crocosphaera watsonii* WH8501: relation to the cell cycle. *Environ. Microbiol.* 14, 967–981. doi: 10.1111/j.1462-2920.2011.02675.x

Falkowski, P. G., Barber, R. T., and Smetacek, V. (1998). Biogeochemical controls and feedbacks on ocean primary production. *Science* 281, 200–207. doi: 10.1126/science.281.5374.200

Finkel, Z. V., Beardall, J., Flynn, K. J., Quigg, A., Rees, T. A. V., Raven, J. A. et al. (2010). Phytoplankton in a changing world: cell size and elemental stoichiometry. *J. Plankton Res.* 32, 119–137. doi: 10.1093/plankt/fbp098

Fu, F. X., Yu, E., Garcia, N. S., Gale, J., Luo, Y. S., Webb, E. A., et al. (2014). Differing responses of marine N_2 fixers to warming and consequences for future diazotroph community structure. *Aquat. Microb. Ecol.* 72, 33–46. doi: 10.3354/ame01683

Garcia, N. S., Fu, F.-X., Breene, C. L., Yu, E. K., Bernhardt, P. W., Mulholland, M. R., et al. (2013). Combined effects of CO2 and light on large and small isolates of the unicellular N_2-fixing *cyanobacterium Crocosphaera watsonii* from the western tropical atlantic ocean. *Eur. J. Phycol.* 48, 128–139. doi: 10.1080/09670262.2013.773383

Großkopf, T., and LaRoche, J. (2012). Direct and indirect costs of dinitrogen fixation in *Crocosphaera watsonii* WH8501 and possible implications for the nitrogen cycle. *Front. Microbiol.* 3:236. doi: 10.3389/fmicb.2012.00236

Hawco, N. J., Fu, F., Yang, N., Hutchins, D. A., and John, S. G. (2020). Independent iron and light limitation in a low-light-adapted *Prochlorococcus* from the deep chlorophyll maximum. *ISME J.* 15, 359–362. doi: 10.1038/s41396-020-00776-y

Held, N. A., Sutherland, K. M., Webb, E. A., McIlvin, M. R., Cohen, N. R., Devaux, A. J., et al. (2020). Mechanisms and heterogeneity of mineral use by natural colonies of the cyanobacterium *Trichodesmium*. *bioRxiv.* 2020:295147. doi: 10.1101/2020.09.24.295147

Huertas, I. E., Rouco, M., López-Rodas, V., and Costas, E. (2011). Warming will affect phytoplankton differently: evidence through a mechanistic approach. *Proc. Royal Society B Biol. Sci.* 278, 3534–3543. doi: 10.1098/rspb.2011.0160

Hutchins, D. A., and Boyd, P. W. (2016). Marine phytoplankton and the changing ocean iron cycle. *Nat. Clim. Chang.* 6:1072. doi: 10.1038/nclimate3147

Hutchins, D. A., and Fu, F. (2017). Microorganisms and ocean global change. *Nat. Microbiol.* 2:17058. doi: 10.1038/nmicrobiol.2017.58

Hutchins, D. A., Fu, F.-X., Webb, E. A., Walworth, N., and Tagliabue, A. (2013). Taxon-specific response of marine nitrogen fixers to elevated carbon dioxide concentrations. *Nat. Geosci.* 6, 790–795. doi: 10.1038/ngeo1858

Inomura, K., Deutsch, C., Wilson, S. T., Masuda, T., Lawrenz, E., Bučinská, L., et al. (2019). Quantifying oxygen management and temperature and light dependencies of nitrogen fixation by *Crocosphaera watsonii*. *mSphere* 4, e519–e531. doi: 10.1128/mSphere.00531-19

IPCC (2014). "Climate Change 2014: Synthesis Report," in *Contribution of Working Groups I, II and III to the Fifth Assessment Report of the Intergovernmental Panel on Climate Change*, eds Core Writing Team. R. K. Pachauri and L. A. Meyer (Geneva, Switzerland: IPCC). 151.

Jabre, L., and Bertrand, E. M. (2020). Interactive effects of iron and temperature on the growth of *Fragilariopsis cylindrus*. *Limnol. Oceanogr. Lett.* 5, 363–370. doi: 10.1002/lol2.10158

Jacq, V., Ridame, C., L'Helguen, S., Kaczmar, F., and Saliot, A. (2014). Response of the unicellular diazotrophic cyanobacterium *Crocosphaera watsonii* to iron limitation. *PLoS One* 9:e86749. doi: 10.1371/journal.pone.0086749

Jiang, H.-B., Fu, F.-X., Rivero-Calle, S., Levine, N. M., Sañudo-Wilhelmy, S. A., Qu, P.-P., et al. (2018). Ocean warming alleviates iron limitation of marine nitrogen fixation. *Nat. Clim. Chang.* 8, 709–712. doi: 10.1038/s41558-018-0216-8

Küpper, H., Šetlík, I., Seibert, S., Prášil, O., Šetlikova, E., Strittmatter, M., et al. (2008). Iron limitation in the marine cyanobacterium *Trichodesmium* reveals new insights into regulation of photosynthesis and nitrogen fixation. *New Phytol.* 179, 784–798. doi: 10.1111/j.1469-8137.2008.02497.x

Kustka, A. B., Sañudo-Wilhelmy, S. A., Carpenter, E. J., Capone, D., Burns, J., Sunda, W. G. et al. (2003). Iron requirements for dinitrogen- and ammonium-supported growth in cultures of *Trichodesmium* (IMS 101): comparison with nitrogen fixation rates and iron: carbon ratios of field populations. *Limnol. Oceanogr.* 48, 1869–1884. doi: 10.4319/lo.2003.48.5.1869

Martiny, A. C., Vrugt, J. A., Primeau, F. W., and Lomas, M. W. (2013). Regional variation in the particulate organic carbon to nitrogen ratio in the surface ocean. *Global Biogeochem. Cycles* 27, 723–731. doi: 10.1002/gbc.20061

Moore, C. M., Mills, M. M., Arrigo, K. R., Berman-Frank, I., Bopp, L., Boyd, P. W., et al. (2013). Processes and patterns of oceanic nutrient limitation. *Nat. Geosci.* 6, 701–710. doi: 10.1038/ngeo1765

Moore, J. K., Doney, S. C., Glover, D. M., and Fung, I. Y. (2001). Iron cycling and nutrient-limitation patterns in surface waters of the world ocean. *Deep Sea Res. Part 2 Top. Stud. Oceanogr.* 49, 463–507. doi: 10.1016/S0967-0645(01)00109-6

Peter, K. H., and Sommer, U. (2013). Phytoplankton cell size reduction in response to warming mediated by nutrient limitation. *PLoS One* 8:e71528. doi: 10.1371/journal.pone.0071528

Raven, J. A., Evans, M. C. W., and Korb, R. E. (1999). The role of trace metals in photosynthetic electron transport in O_2-evolving organisms. *Photosynth. Res.* 60, 111–150. doi: 10.1023/A:1006282714942

Raven, J. A., and Geider, R. J. (1988). Temperature and algal growth. *New Phytol.* 110, 441–461. doi: 10.1111/j.1469-8137.1988.tb00282.x

Roche, J. L., Boyd, P. W., McKay, R. M. L., and Geider, R. J. (1996). Flavodoxin as an *in situ* marker for iron stress in phytoplankton. *Nature* 382:802. doi: 10.1038/382802a0

Saito, M. A., Bertrand, E. M., Dutkiewicz, S., Bulygin, V. V., Moran, D. M., Monteiro, F. M., et al. (2011). Iron conservation by reduction of metalloenzyme inventories in the marine diazotroph *Crocosphaera watsonii*. *Proc. Natl. Acad. Sci. U S A.* 108, 2184–2189. doi: 10.1073/pnas.1006943108

Schoffman, H., Lis, H., Shaked, Y., and Keren, N. (2016). Iron–nutrient interactions within phytoplankton. *Front. Plant Sci.* 7:1223. doi: 10.3389/fpls.2016.01223

Sohm, J. A., Webb, E. A., and Capone, D. G. (2011). Emerging patterns of marine nitrogen fixation. *Nat. Rev. Microbiol.* 9, 499–508. doi: 10.1038/nrmicro2594

Sunda, W. G., Price, N. M., and Morel, F. M. M. (2005). Trace metal ion buffers and their use in culture studies. *Algal Cult. Techniq.* 2005, 35–63. doi: 10.1016/b978-012088426-1/50005-6

Thomas, M. K., Kremer, C. T., Klausmeier, C. A., and Litchman, E. (2012). A global pattern of thermal adaptation in marine phytoplankton. *Science* 338:1085. doi: 10.1126/science.1224836

Tovar-Sanchez, A., Sañudo-Wilhelmy, S. A., Garcia-Vargas, M., Weaver, R. S., Popels, L. C., Hutchins, D. A., et al. (2003). A trace metal clean reagent to remove surface-bound iron from marine phytoplankton. *Mar. Chem.* 82, 91–99. doi: 10.1016/S0304-4203(03)00054-9

Webb, E. A., Ehrenreich, I. M., Brown, S. L., Valois, F. W., and Waterbury, J. B. (2009). Phenotypic and genotypic characterization of multiple strains of the diazotrophic cyanobacterium, *Crocosphaera watsonii*, isolated from the open ocean. *Environ. Microbiol.* 11, 338–348. doi: 10.1111/j.1462-2920.2008.01771.x

Zehr, J. P., and Capone, D. G. (2020). Changing perspectives in marine nitrogen fixation. *Science* 368:eaay9514. doi: 10.1126/science.aay9514

Zehr, J. P., Waterbury, J. B., Turner, P. J., Montoya, J. P., Omoregie, E., Steward, G. F., et al. (2001). Unicellular cyanobacteria fix N_2 in the subtropical north pacific ocean. *Nature* 412, 635–638. doi: 10.1038/35088063

Conflict of Interest: The authors declare that the research was conducted in the absence of any commercial or financial relationships that could be construed as a potential conflict of interest.